

1. Background and Motivation

Currently, few models exist that successfully incorporate three co-circulating (sub)types of influenza in tropical settings [1]. Tropical settings are a unique situation for influenza dynamics because epidemics do not occur with consistent timing, often occurring at points throughout the year with inconsistent timings between epidemics [2,3]. Therefore, we aimed here to parameterize models for influenza dynamics in tropical settings that can incorporate three (sub)types and non-annual incidence patterns. This can be used for various research purposes such as evaluating potential etiological factors leading to epidemics or management policies such as vaccination [4].

Providing parameterizations for these models through a parameter search rather than through model fitting avoids the likely overfitting that would result from model fitting. Previous research has shown that fitting three (sub)type models without strong cyclic patterns in incidence is challenging and likely requires overfitting or poor-quality fits. Here we provide parameterizations for multiple forms of a mathematical model that can emulate the influenza dynamics seen in tropical world regions.

2. Model Specification

The model applies SIRS dynamics to all three cocirculating (sub)types, allowing infected and recovered compartments for each individual (sub)type. The model runs for a ten-year period following a ten-year “burn-in” period to avoid major fluctuations commonly seen during the first years in an epidemic model. We applied a two-stage infected class and various multi-stage recovered classes to allow durations of infection and immunity to be Erlang distributed [5]. Infected individuals can be hospitalized, and a subset of hospitalized cases are fatal. Infection with one (sub)type confers partial immunity to the others. The model includes eight decade-based age classes, ranging between 0-9 years to 70+. The initial total model population is one million individuals, with an age structure based on data from Vietnam [6]. The model includes natural birth and death.

Due to some uncertainty regarding true influenza dynamics in tropical regions and what factors may contribute to nonannual incidence patterns, we considered three ways to vary the form of our model: multi-stage recovery classes, introduction of subpopulations, and case importation. To incorporate multi-stage recovery, we considered two, four, and six recovery classes across (sub)types. To incorporate subpopulations, we considered a single population, two populations of equal size, and two populations of unequal size (80/20 population ratio). To incorporate importation, we considered models with and without periodic seeding of a susceptible individual into an infected compartment. Among these variations (three forms of multi-stage recovery, three forms of subpopulation, and two options for importation), 18 total model configurations exist.

In addition to parameters estimated through parameter-space search, some parameters were assumed constant for consistency across models. The relative age structure within the model was based on data from published age demographics for Vietnam [6]. The crude birth rate, μ , was reported by the World Bank [7], and the age-based natural death rate was reported by the World Health Organization [8]. Age-based contact mixing within a population, denoted η_{ij} between age groups i and j , was incorporated through previously estimated age-based contact patterns for Vietnam [9,10]. Duration of infection, ν^{-1} , was assumed to be five days. Age-based probabilities of hospitalization and death if hospitalized, denoted h and d respectively, were taken from published data from the United States Centers for Disease Control and Prevention [11].

Parameters that were included in the parameter-space search include the transmission rate for each (sub)type, denote β_s for (sub)type s , with the assumed ordering of $\beta_B < \beta_{H1} < \beta_{H3}$. The duration of immunity following infection (ρ^{-1}), in days, was assumed to be the same across (sub)types and estimated. Quantities of cross immunity (σ_{ij}), defined as reductions in transmissibility following infection with any (sub)type to the others, were estimated for each pair, assumed to be symmetric. For models that include two subpopulations, two mixing parameters (ξ_{12} and ξ_{21}) were incorporated and estimated to denote the relative amount of mixing across populations compared to within-population

mixing. Including two parameters allows asymmetry. For models that include importation, the frequency of importation, in days, was estimated.

The following equations illustrate the model with four recovery classes, one population, and no importation. These equations are easily modifiable to apply to the other model forms we considered. The model is also shown in the diagram in Figure 1, and parameters used are shown in Table 1.

$$\begin{aligned}
\frac{dS_{\tilde{a}}}{dt} &= \mu_{\tilde{a}} - \sum_a \sum_s \eta_{a\tilde{a}} \beta_s S_{\tilde{a}} (I_{as}^1 + I_{as}^2) + \sum_s \frac{\rho}{4} R_{\tilde{a}s}^4 \\
\frac{dI_{\tilde{a}\tilde{s}}^1}{dt} &= \sum_a \eta_{a\tilde{a}} \beta_{\tilde{s}} S_{\tilde{a}} (I_{a\tilde{s}}^1 + I_{a\tilde{s}}^2) + \sum_a \sum_{s \neq \tilde{s}} \sum_{i=1}^4 \eta_{\tilde{a}a} \beta_{\tilde{s}} \sigma_{\tilde{s}s} R_{\tilde{a}s}^i (I_{a\tilde{s}}^1 + I_{a\tilde{s}}^2) - \frac{h\nu}{2} I_{\tilde{a}\tilde{s}}^1 - \frac{(1-h)\nu}{2} I_{\tilde{a}\tilde{s}}^1 \\
\frac{dI_{\tilde{a}\tilde{s}}^2}{dt} &= \frac{(1-h)\nu}{2} I_{\tilde{a}\tilde{s}}^1 - \frac{\nu}{2} I_{\tilde{a}\tilde{s}}^2 \\
\frac{dH_{\tilde{a}\tilde{s}}}{dt} &= \frac{h\nu}{2} I_{\tilde{a}\tilde{s}}^1 - \frac{d\nu}{2} H_{\tilde{a}\tilde{s}} - \frac{(1-d)\nu}{2} H_{\tilde{a}\tilde{s}} \\
\frac{dR_{\tilde{a}\tilde{s}}^1}{dt} &= \frac{\nu}{2} I_{\tilde{a}\tilde{s}}^2 + \frac{(1-d)\nu}{2} H_{\tilde{a}\tilde{s}} - \frac{\rho}{4} R_{\tilde{a}\tilde{s}}^1 - \sum_a \sum_{s \neq \tilde{s}} \eta_{a\tilde{a}} \beta_s \sigma_{\tilde{s}s} R_{\tilde{a}\tilde{s}}^1 (I_{as}^1 + I_{as}^2) \\
\frac{dR_{\tilde{a}\tilde{s}}^i}{dt} &= \frac{\rho}{4} R_{\tilde{a}\tilde{s}}^{i-1} - \frac{\rho}{4} R_{\tilde{a}\tilde{s}}^i - \sum_a \sum_{s \neq \tilde{s}} \eta_{a\tilde{a}} \beta_s \sigma_{\tilde{s}s} R_{\tilde{a}\tilde{s}}^i (I_{as}^1 + I_{as}^2), i \in \{2, 3, 4\}
\end{aligned}$$

where \tilde{a} denotes any particular age group and \tilde{s} denotes any particular (sub)type of influenza.

3. Parameter Search

For the parameters that we estimated through parameter-space search, we used a form of Approximate Bayesian Computation. We set prior distributions for each parameter and drew sets of all parameters.

For each drawn set of parameters, we assessed whether they produce influenza dynamics resembling those seen in tropical regions (cocirculating subtypes, nonannual cycles). We

assessed this by evaluating a set of seven criteria based on observed influenza dynamics in Vietnam. These criteria are:

- i) Standard deviation of daily incidence for each (sub)type is greater than 100 in a population of one million
- ii) All pairwise correlations between daily incidence values of pairs of (sub)types are less than 0.7 in absolute value.
- iii) Among the maximum daily incidence values for each (sub)type, the lowest maximum value is no less than 80% of the highest maximum value.
- iv) The maximum daily incidence values among each (sub)type in each five-year period span at least 100 days.
- v) Ratios of selected quantile pairs (10th, 25th, 75th, and 90th percentiles) from daily incidence values match those observed in the data from Vietnam within a tolerance of 33%.
- vi) Annual all-influenza attack rates range between 15 and 35%.
- vii) Annual all-influenza attack rates do not monotonically increase or decrease over the ten-year period.

Figure 1. Model diagram for a model with one population, four recovery classes, and no importation. The diagram shows the compartments available for all eight age classes.

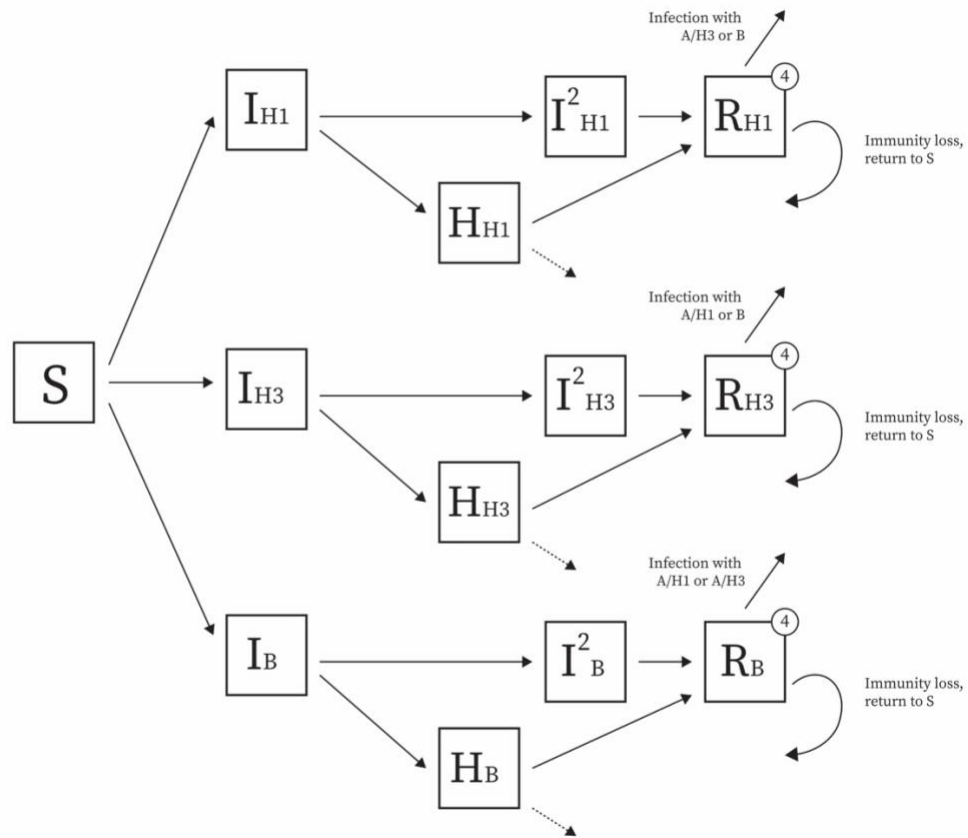


Table 1. Parameters assumed, taken from literature, and estimated for mathematical model, including references for values or methods of estimation.

Parameter	Value	Reference or method of estimation
transmission parameter for A/H1, β_{H1}	Estimated in parameter search	Middle value after drawing 1. $\mu_\beta \sim U(0.15, 0.70)$ 2. 3 Draws of $N(\mu_\beta, 0.01)$
transmission parameter for A/H3, β_{H3}	Estimated in parameter search	Highest value after drawing 1. $\mu_\beta \sim U(0.15, 0.70)$ 2. 3 Draws of $N(\mu_\beta, 0.01)$
transmission parameter for B, β_B	Estimated in parameter search	Lowest value after drawing 1. $\mu_\beta \sim U(0.15, 0.70)$ 2. 3 Draws of $N(\mu_\beta, 0.01)$
Cross immunity across (sub)types, σ_{ij}	Estimated in parameter search	Each drawn from $U(0, 1)$
Mixing across age groups, η_{ij}	Asymmetric contact matrix	[10]
Duration between case importations	Estimated in parameter search	Drawn from $U(90, 365)$
Duration of infection (days), ν^{-1}	5	Assumed
Hospitalization fraction among cases, all (sub)types, h	0-9: 0.0048 10-19: 0.0033 20-29: 0.0056 30-39: 0.0056 40-49: 0.0056 50-59: 0.0106 60-69: 0.0460 70+: 0.0909	[11]
Death fraction among hospitalizations, all (sub)types, d	0-9: 0.0094 10-19: 0.0125 20-29: 0.0289 30-39: 0.0289 40-49: 0.0289 50-59: 0.0574 60-69: 0.0780 70+: 0.1041	[11]
Duration of infection-induced immunity (days), ρ^{-1}	Estimated in parameter search	Drawn from $U(180, 1460)$
Natural birth or aging rate, μ	15 births per 1,000 population annually	[7]
Relative mixing across subpopulations, ξ_{ij}	Estimated	Drawn from $U(0, 1)$

References

1. Yang W, Lau EHY, Cowling BJ. Dynamic interactions of influenza viruses in Hong Kong during 1998-2018. *PLoS Comput Biol*. 2020 Jun 15;16(6).
2. Lam HM, Wesolowski A, Hung NT, Nguyen TD, Nhat NTD, Todd S, et al. Nonannual seasonality of influenza-like illness in a tropical urban setting. *Influenza Other Respir Viruses*. 2018;12(6):742–54.
3. Servadio JL, Thai PQ, Choisy M, Boni MF. Repeatability and timing of tropical influenza epidemics. *PLOS Comput Biol*. 2023 Jul 19;19(7):e1011317.
4. Servadio JL, Choisy M, Thai PQ, Boni MF. Influenza vaccination allocation in tropical settings under constrained resources. *MedRxiv Prepr Serv Health Sci*. 2024 Feb 9;2024.02.08.24302551.
5. Lloyd AL. Realistic Distributions of Infectious Periods in Epidemic Models: Changing Patterns of Persistence and Dynamics. *Theor Popul Biol*. 2001 Aug 1;60(1):59–71.
6. Vietnam Population 2023 [Internet]. World Population Review. [cited 2023 Aug 3]. Available from: <https://worldpopulationreview.com/countries/vietnam-population>
7. World Bank. Birth rate, crude (per 1,000 people) - Vietnam [Internet]. World Bank Open Data. [cited 2023 Sep 12]. Available from: <https://data.worldbank.org/indicator/SP.DYN.CBRT.IN?locations=VN>
8. World Health Organization. Life tables: Life tables by country Viet Nam [Internet]. Regional Health Observatory - South East Asia. 2020 [cited 2023 Sep 7]. Available from: <https://apps.who.int/gho/data/view.searo.61830?lang=en>
9. Prem K, Zandvoort K van, Klepac P, Eggo RM, Davies NG, Group C for the MM of IDC 19 W, et al. Projecting contact matrices in 177 geographical regions: An update and comparison with empirical data for the COVID-19 era. *PLOS Comput Biol*. 2021 Jul 26;17(7):e1009098.
10. Prem K. kishaprem/synthetic-contact-matrices: First release of the synthetic contact matrices repository [Internet]. Zenodo; 2021 [cited 2023 Sep 13]. Available from: <https://zenodo.org/record/4889500>
11. Centers for Disease Control and Prevention. Estimated Flu-Related Illnesses, Medical visits, Hospitalizations, and Deaths in the United States — 2018–2019 Flu Season [Internet]. 2021 [cited 2023 Aug 3]. Available from: <https://www.cdc.gov/flu/about/burden/2018-2019.html>